# Neurocalcin δ Modulation of ROS-GC1, a New Model of $Ca^{2+}$ Signaling†

Venkateswar Venkataraman,‡,§ Teresa Duda,‡,|| Sarangan Ravichandran,⊥ and Rameshwar K. Sharma*,||

*The Unit of Regulatory and Molecular Biology, Division of Biochemistry and Molecular Biology, Pennsylvania College of Optometry, Elkins Park, Pennsylvania 19027, Department of Cell Biology, UMDNJ-SOM, Stratford, New Jersey 08084, and Advanced Biomedical Computing Center, National Cancer Institute, SAIC/Frederick, Frederick, Maryland 21702*

*Received March 6, 2008; Revised Manuscript Received April 23, 2008*

ABSTRACT: ROS-GC1 membrane guanylate cyclase is a $Ca^{2+}$ bimodal signal transduction switch. It is turned "off" by a rise in free $Ca^{2+}$ from nanomolar to the semicromolar range in the photoreceptor outer segments and the olfactory bulb neurons; by a similar rise in the bipolar and ganglion retinal neurons it is turned "on". These opposite operational modes of the switch are specified by its $Ca^{2+}$ sensing devices, respectively termed GCAPs and CD-GCAPs. Neurocalcin δ is a CD-GCAP. In the present study, the neurocalcin δ-modulated site, $V^{837}-L^{858}$, in ROS-GC1 has been mapped. The location and properties of this site are unique. It resides within the core domain of the catalytic module and does not require the α-helical dimerization domain structural element (amino acids 767−811) for activating the catalytic module. Contrary to the current beliefs, the catalytic module is intrinsically active; it is directly regulated by the neurocalcin δ-modulated $Ca^{2+}$ signal and is dimeric in nature. A fold recognition based model of the catalytic domain of ROS-GC1 was built, and neurocalcin δ docking simulations were carried out to define the three-dimensional features of the interacting domains of the two molecules. These findings define a new transduction model for the $Ca^{2+}$ signaling of ROS-GC1.

The seminal discoveries of the membrane guanylate cyclases ANF-RGC[1] (*1–3*) and ROS-GC (*4, 5*) opened two new transduction chapters of the cyclic GMP signaling pathways (reviewed in refs *6–9*). The first established that the hormonally dependent membrane guanylate cyclase transduction mechanism is distinct from the G-protein-coupled receptors and the soluble guanylate cyclases and, importantly, ceased the intense debate that questioned the independent integrity of its operation. With subsequent findings of two other receptor membrane guanylate cyclases (*10–12*), a new issue came to the forefront.

Is the receptor guanylate cyclase family sole representative of all members of the family, meant only to transduce the hormone signals, generated outside the cell?

In the second chapter, with the discovery of ROS-GC, the issue was resolved, and the answer was no. ROS-GC was the source of cyclic GMP that was the intracellular messenger of the LIGHT signal. It was solely modulated by the intracellular pulsated levels of $Ca^{2+}$ within the photoreceptors (*13*).

With these observations, the membrane guanylate cyclase family branched into two subfamilies, hormone receptor and $Ca^{2+}$-modulated, and importantly, the family got the recognition of being the transducer of both types of signals, generated outside and inside the cells (reviewed in refs *6, 9*).

At present, the field is in its third phase. The currently debated issue is: Is the ROS-GC transduction mechanism in the exclusive domain of the outer segments of rods and cones solely linked with phototransduction? Based on emerging evidence, the answer is no. Studies with the selected systems demonstrate that the ROS-GC transduction system spans across the entire neural network linked with the senses of vision (*14–16*), smell (*17–19*), and taste (*20*). It is also present in the hippocampus (*21*) and pinealocytes (*22*) and in a non-neuronal system of the seminiferous tubules (*23*).

ROS-GC is a two-component transduction system: the $Ca^{2+}$ sensor component, GCAP (guanylate cyclase activating protein) or CD- ($Ca^{2+}$-dependent) GCAP, and the transducer component, ROS-GC membrane guanylate cyclase. Two forms of GCAP, 1 and 2, are expressed across species (*24–27*); in addition, cones of human and zebrafish also contain GCAP3 (*28*). Upon sensing progressive rises in free $Ca^{2+}$, GCAPs proportionately decelerate the ROS-GC activity. CD-GCAP exists in three forms: S100B, neurocalcin δ, and frequenin (*21, 29–32*). They accelerate the ROS-GC activity.

ROS-GC exists in three forms: ROS-GC1 (*4, 5*), ROS-GC2 (*33, 34*), and ONE-GC (*17, 35*). Thus, theoretically, with individual pairing of a GCAP with each ROS-GC, the GCAP-modulated ROS-GC transduction machine can exist in multiple forms; three have been characterized in the retinal

† This study was supported by NIH Grants DC005349 (R.K.S.), HL070015, and HL 084584 (T.D.) and the UMDNJ and Lindback Foundation (V.V.).

* To whom correspondence should be addressed: phone, 215-780-3124; fax, 215-780-3125; e-mail, rsharma@pco.edu.

‡ These authors contributed equally to this work.

§ UMDNJ-SOM.

|| Pennsylvania College of Optometry.

⊥ National Cancer Institute.

[1] Abbreviations: ANF-RGC, atrial natriuretic factor receptor membrane guanylate cyclase; catcd, catalytic core domain; catd, catalytic domain; CD-GCAP, calcium-dependent guanylate cyclase activating protein; dd, dimerization domain; GCAP, guanylate cyclase activating protein; khd, kinase homology domain; ONE-GC, olfactory neuroepithelial membrane guanylate cyclase; ROS-GC, rod outer segment membrane guanylate cyclase.

10.1021/bi800394s CCC: $40.75 
Published on Web 05/24/2008

neurons (*25, 33, 36, 37*), one in the olfactory bulb (*38*), and one in the pinealocytes (*22*). Similarly, paired with a CD-GCAP, it can exist in multiple forms. S100B-modulated ROS-GC1 is present in the photoreceptor-bipolar synapse (*14*), the pinealocytes (*22*), and gustatory epithelium (*20*); neurocalcin δ-modulated ROS-GC1, in the inner retinal neurons (*16*); ONE-GC, in the olfactory neuroepithelium (*17*); and frequenin-modulated ONE-GC, in hippocampal neurons (*21*). Remarkably, GCAP1, an inhibitory $Ca^{2+}$ sensor of ROS-GC1 in photoreceptors, is a stimulatory $Ca^{2+}$ sensor of ONE-GC in the olfactory neuroepithelium (*39*).

This raises an important physiological issue: How does ROS-GC1 achieve cellular specificity for the diverse $Ca^{2+}$ signals?

Ongoing studies indicate that this is accomplished through the elegant structural designs of the GCAPs/CD-GCAPs and of the domains of ROS-GC1, which they modulate. Each ROS-GC1 module is crafted to fit with only a single $Ca^{2+}$ sensor, and upon their union the module attains an independent status of being a sole messenger of GCAP- or CD-GCAP-transmitted $Ca^{2+}$ signals. In this manner, at one time, only one type of the $Ca^{2+}$ signal controls the activity of the catalytic module of ROS-GC1. The net result is that each $Ca^{2+}$ spike is faithfully translated into the production of cyclic GMP by ROS-GC and cyclic GMP via its downstream signaling components precisely controls cellular activity.

The present study was undertaken to gain an in-depth structural understanding of the mechanism by which the neurocalcin δ module regulates $Ca^{2+}$ signaling of ROS-GC1. The findings reveal a new paradigm of $Ca^{2+}$ signaling, redefine the catalytic module boundary of ROS-GC1, and demonstrate a set of new principles by which the catalytic module of ROS-GC1 operates. These principles are contrary to the current beliefs.

## MATERIALS AND METHODS

*ROS-GC1 Mutants.* Domain structures of ROS-GC1 mutants used in this study are schematically represented in Figures 1A and 2A. The membrane-bound mutants, Δ1016−1054, Δ972−1054, and Δ965−1054 (Δcte), and the soluble construct, $M^{733}$−$K^{1054}$, were prepared as described earlier (*14*).

The soluble constructs $L^{806}$−$T^{986}$ and $G^{817}$−$Y^{965}$ of ROS-GC1 were obtained through PCR amplification of bovine ROS-GC1 cDNA. The catcd mutant lacking the $^{844}$MSEPIE$^{849}$ motif (catcdΔMSEPIE) was prepared using the QuickChange mutagenesis kit (Stratagene). These fragments were cloned into pET30aLIC vector, expressed in *Escherichia coli*, and purified on a Ni-NTA column (*16*).

*Expression and Guanylate Cyclase Activity Assay.* COS-7 cells were transfected with the appropriate expression construct through standard procedures. Sixty hours after transfection, the cells were washed with 50 mM Tris-HCl (pH 7.5)/10 mM $MgCl_2$ buffer, scraped into cold buffer, homogenized, centrifuged at 5000*g*, and washed with the same buffer. The pellet represented crude membranes. The guanylate cyclase activity was assessed according to the previous protocols (*39, 40*).

*Peptide Competition Experiments.* Membranes of COS cells expressing ROS-GC1 were incubated with 2 μM neurocalcin δ, 100 μM $CaCl_2$, and increasing concentrations of peptides for 10 min at 37 °C and assayed for guanylate cyclase activity.

*Expression and Purification of Neurocalcin δ.* Myristoylated neurocalcin δ was expressed in *E. coli* and purified as in ref *16*.

*Surface Plasmon Resonance (SPR) Measurements.* The purified ROS-GC1 fragment [150 ng/μL in 50 mM sodium acetate (pH 4.0)] was immobilized on a CM5 sensor chip. The amount of immobilized protein was ∼0.4 ng/mm$^2$. An independent flow cell was subjected to a "blank immobilization" (no protein) and used as control. The running buffer contained 10 mM Tris-HCl (pH 7.5), 150 mM NaCl, 2 mM $CaCl_2$, and 0.005% surfactant P20. The purified, myristoylated neurocalcin δ was diluted in the same buffer and injected into the flow cell (the flow rate was 10 μL/min). The curves were fitted according to a 1:1 Langmuir model.

*Molecular Modeling.* The three-dimensional structure of the ROS-GC1's dimeric core catalytic module (catcd), $G^{817}$−$Y^{965}$, was modeled using the Phyre program (*42*; details in http://www.sbg.bio.ic.ac.uk/∼phyre/). To identify the correct fold for the query sequence, this program uses profile−profile matching methods together with the secondary structure predictions. The profile [position-specific scoring matrix (PSSM)] (*42*) of the query sequence is derived from a multiple sequence alignment of the hits in a position-specific iterative blast (PSI-BLAST) search.

The search using the catcd sequence identified a PDB entry 1AZS (chains a and b) as a possible fold for the catcd with *E*-values/estimated precision (%) as 2.0e−19/100 and 2.9e−18/100, respectively. The Phyre models based on 1AZS (chain a and b) were assembled to form the catcd dimer structure. Accelrys Discovery Studio 1.7 program was used to add hydrogens to the amino acid residues and energy minimized using the CHARMm force field with a small harmonic restraint of force constant 20 kcal (mol Å$^2$)$^{-1}$. The harmonic restraint was added to preserve the fold. The Adopted Basis Newton−Raphson (ABNR) algorithm was used for energy minimization with rms gradient of 0.1 kcal (mol Å)$^{-1}$. Residues present at the dimer interface are listed in the Supporting Information.

Docking was carried out as described in the Supporting Information.

## RESULTS

*Neurocalcin δ-Modulated Domain in ROS-GC1 Resides within the aa733−963 Region.* Reconstitution studies with ROS-GC1 deletion and hybrid constructs have demonstrated that the fragment aa733−1054 is composed of three distinct $Ca^{2+}$ signaling modules, one modulated by GCAP2, the second by S100B, and the third by neurocalcin δ (*14, 32, 43*). Through the process of elimination it was inferred that the neurocalcin δ-modulated domain in ROS-GC1 resides in the aa733−963 segment (*16*), an inference supported now by the following study.

Three ROS-GC1 deletion mutants, Δ1016−1054, Δ972−1054, and Δ965−1054 (Δcte) (Figure 1A), were constructed, expressed in COS cells, and assessed for their basal and neurocalcin δ-dependent guanylate cyclase activities at a fixed, 100 μM, $Ca^{2+}$ concentration; membranes expressing wild-type ROS-GC1 served as controls. The basal activity of the mutants was comparable to each other and to the wild

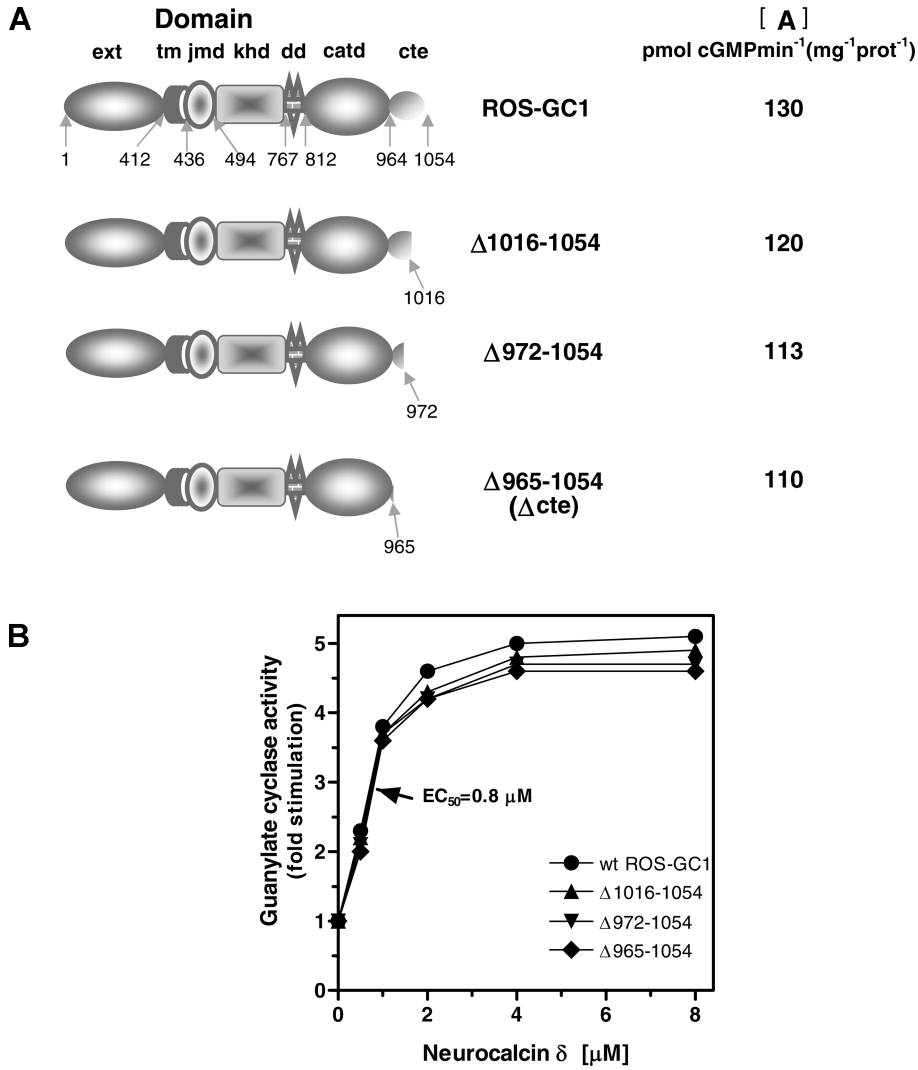


FIGURE 1: Mapping of the neurocalcin $\delta$-modulated region. (A) Schematic representation of ROS-GC1 and its deletion mutants. The following abbreviations denote the predicted domains: ext, extracellular domain; tm, transmembrane domain; jmd, juxtamembrane domain; khd, kinase homology domain; dd, dimerization domain; catd, cyclase catalytic domain; cte, C-terminal extension. Numbering corresponds to the mature protein. Specific activities of the proteins are shown in the right-hand column ([A]). (B) Neurocalcin $\delta$-dependent stimulation of ROS-GC1 and its deletion derivatives. COS cells were individually transfected with ROS-GC1 or its deletion mutant cDNA, and the cell particulate fractions were prepared. These were assayed for guanylate cyclase activity in the presence of incremental concentrations of neurocalcin $\delta$ and 100 $\mu$M $Ca^{2+}$. The experiment was done in triplicate and repeated two times. The results presented are from one typical experiment. Error bars are within the size of the symbols.

type [110−130 pmol of cyclic GMP $min^{-1}$ (mg of protein)$^{-1}$ (Figure 1A)], indicating that all were equally expressed and the deleted fragments had no deleterious effect on their structural integrities.

The wild-type ROS-GC1 and its truncated mutants responded to neurocalcin $\delta$ in a dose-dependent fashion and with almost identical patterns; their half-maximal ($EC_{50}$) activations occurred at 0.8 $\mu$M and saturations at about 4 $\mu$M (Figure 1B). Collectively, these results prove that the cte domain of ROS-GC1, aa965−1054, has no role in the neurocalcin $\delta$ modulation of $Ca^{2+}$ signaling, and also, it is not involved in controlling the basal activity of ROS-GC1. Therefore, the neurocalcin $\delta$-modulated domain must reside in the aa733−964 fragment of ROS-GC1.

These results support the earlier inference but do not directly prove that the ROS-GC1 segment, aa733−964, houses the neurocalcin-modulated site. It was proven by the following studies.

*The Neurocalcin δ-Modulated Site Resides in the Core Catalytic Domain, and This Domain Lacks the α-Helical Dimerization Structural Element*. The aa733−964 segment of ROS-GC1 is composed of the following sequential domains: partial kinase homology domain (khd), aa733−766; α-helical dimerization domain (dd), aa767−811; catalytic domain (catd), aa812−964 (Figure 2A). Their percentage sequence identities with the corresponding domains of ROS-GC2 and ONE-GC are as follows: partial khd, 63 and 49; dd, 91 and 76; catd, 92 and 85. It is noted that the boundaries of the dd and the catd are arbitrary and have not yet been properly defined experimentally.

Because the khd segment is the least conserved and catd the most conserved, the initial intuition was that the khd segment, aa737−766, might represent the neurocalcin $\delta$-modulated domain. This possibility was tested by the use of a soluble construct, $L^{806}$−$T^{986}$ (Figure 2A). This construct lacked the khd segment, aa733−766, and, notably, also the dd. The selection of this construct was based on the consideration that it will segregate the catalytic domain from the domain that houses the neurocalcin $\delta$-modulated domain. The decision to assign the $L^{806}$−$T^{986}$ boundary to the catd

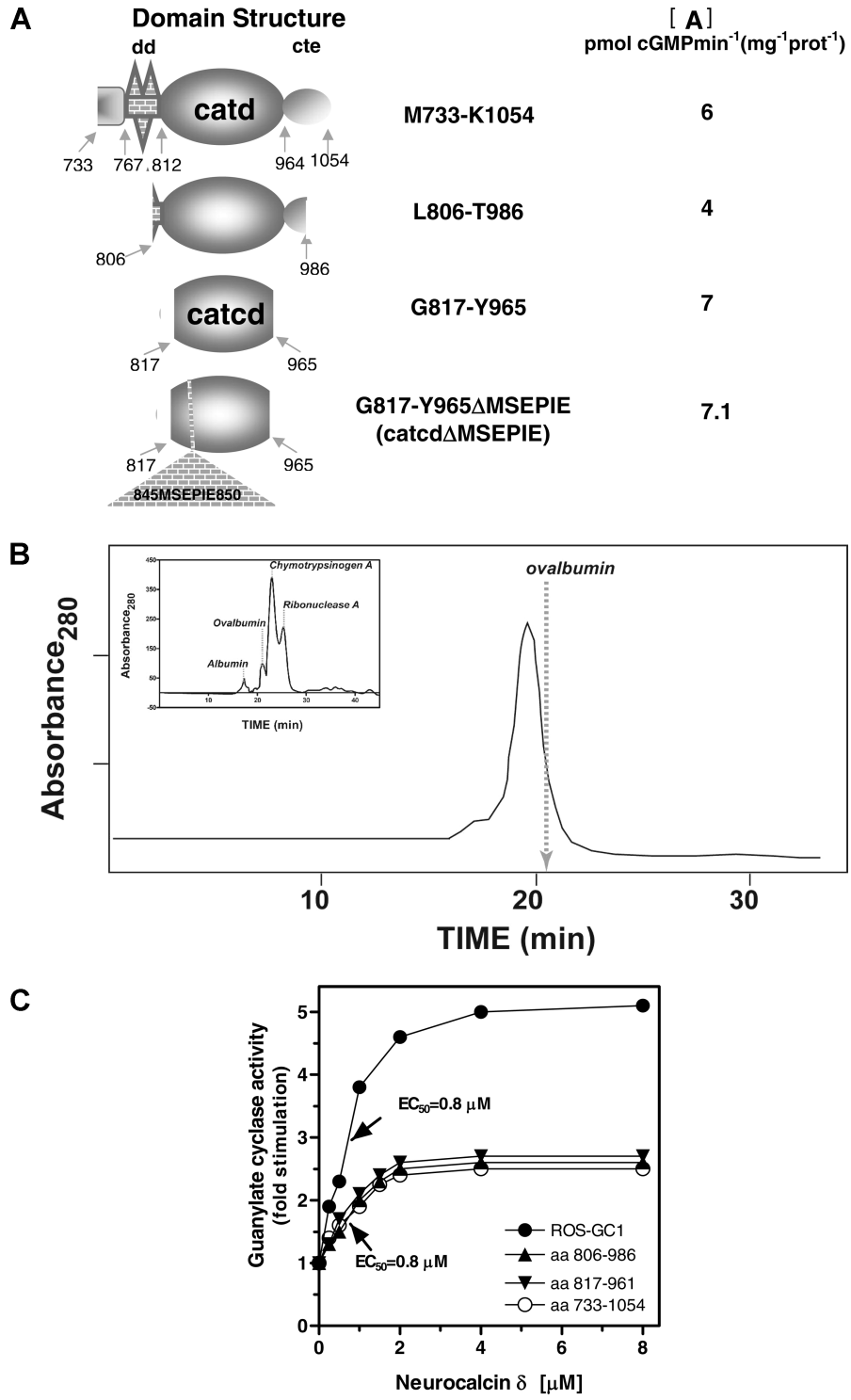


FIGURE 2: The neurocalcin δ interaction site with ROS-GC1 resides within the ROS-GC1 domain $G^{817}-Y^{965}$. (A) Schematic representation of the ROS-GC1 soluble fragments. The following abbreviations denote the predicted domains: dd, dimerization domain; catd, cyclase catalytic domain; catcd; catalytic core domain; cte, C-terminal extension. Numbers shown correspond to the mature protein. Specific activity of the fragments is given in the right-hand column ([A]). (B) Analysis of the purified catcd domain by gel filtration. The ROS-GC1 catcd domain was expressed in *E. coli* and purified. The purified protein was loaded onto a Superdex 75 gel filtration column and analyzed on an Akta FPLC system. Loading and elution was in buffer containing 220 mM Tris-HCl (pH 7.5) and 150 mM NaCl. Elution was monitored by absorbance at 280 nm. A single peak was observed with a retention time of 19.4 min, corresponding to a size of 50 kDa. The column was calibrated using molecular size standards purchased from Amersham Biosciences. The retention time for one of the standards, ovalbumin, is indicated by a gray dashed arrow. Inset: The elution profile of the standards used is shown; the peak corresponding to each protein standard is labeled. The experiment was carried out with three separate preparations of the protein. The results presented are from one experiment. (C) Stimulation of the soluble ROS-GC1 fragments by neurocalcin δ. ROS-GC1 fragments aa733−1054, aa806−986, or aa817−965 were expressed and purified. These proteins were tested for neurocalcin δ-dependent cyclase activity in the presence of 100 μM $Ca^{2+}$. The experiment was repeated two times with separate preparations of the protein. Error bars are within the size of the symbols.

was that this domain is conserved among all members of the membrane guanylate cyclase family, and there is even higher conservation among the ROS-GC subfamily members, 92% with ROS-GC2 and 85% with ONE-GC. Because the

core domain of the catd (catcd) has not been clearly defined (*44, 45*), as a precautionary measure not to disturb its functional integrity, the design of the $L^{806}-T^{986}$ construct was such that its boundary extended into the cte domain. This strategy was based on the original information from the surface receptor membrane guanylate cyclase subfamily where the catalytic domain stretched and ended at the C-terminal end. Importantly, because the $L^{806}-T^{986}$ fragment did not contain dd, it was expected that this domain will be monomeric and will have no intrinsic and regulatory activity. Earlier studies had demonstrated that dd is obligatory for the signal transduction activity of all membrane guanylate cyclases (*44, 46, 47*). The predicted function of dd is to form the contact points for homodimerization of the catalytic module and bring this module from the inactive to the active state.

The $L^{806}-T^{986}$ and other soluble constructs represented in Figure 2A were expressed in *E. coli* and purified to homogeneity. All were biologically active; they contained comparable intrinsic guanylate cyclase activity (Figure 2A), and as it will become clear, they were significantly stimulated by neurocalcin δ. A noteworthy point is that the intrinsic guanylate cyclase activities of all soluble constructs were about 20-fold lower than the membrane-bound constructs (compare Figures 1A and 2A). This difference in activities has also been observed before for other soluble constructs of the membrane guanylate cyclases (*16, 48*), yet it has not been commented upon. It is now noted that the difference is accountable to the transmembrane module, which apparently upregulates the catalytic module activity (*19*).

These results demonstrate that the α-helical dd is not a part of the catcd and catcd by itself has an intrinsic catalytic activity.

To assess the oligomeric status of catcd, gel filtration analysis was carried out. The purified protein was loaded onto a Superdex 75 column, and the eluted fractions were monitored by absorbance at 280 nm. A single peak with a retention time of 19.4 min was observed (Figure 2B). On the basis of calibration with molecular mass standards (Figure 2B, inset) this peak corresponded to the 50 kDa protein, indicating that the catcd exists as a dimer in its isolated form.

*The Catcd Segment $L^{806}-T^{986}$ Contains the Neurocalcin δ-Modulated Site.* The reconstitution experiment where the $L^{806}-T^{986}$ fragment of ROS-GC1 and neurocalcin δ were the sole components demonstrated that, in the presence of the saturation amount of free $Ca^{2+}$, neurocalcin δ stimulated the guanylate cyclase activity in a dose-dependent fashion (Figure 2C). This mode and extent of the guanylate cyclase stimulation were almost identical to those of the parent mutant, representing its aa733−1054 fragment (Figure 2C). In both cases the $EC_{50}$ value of neurocalcin δ was 0.8 μM; $V_{max}$ was achieved at about 2 μM, and maximal stimulation was about 2.5-fold (Figure 2C). These results demonstrate that $L^{806}-T^{986}$ contains the neurocalcin δ-modulated site and that the partial khd fragment, dd, and cte segments in the aa733−1054 domain of ROS-GC1 have no relationship with the neurocalcin δ-modulated domain. Thus, this evidence pointed to the catcd for housing the neurocalcin-modulated domain. Therefore, the $G^{817}-Y^{965}$ mutant, catcd, became the subject of investigation.

The catcd is a highly conserved domain between the membrane guanylate cyclase family members; there is 93% sequence similarity with its corresponding domain in ROS-GC2 and more than 85% with ONE-GC. It was, therefore, predicted that catcd represents the core domain of the catalytic module.

A reconstitution experiment showed that the $G^{817}-Y^{965}$ mutant's mode of response to neurocalcin δ was identical to that of the $L^{806}-T^{986}$ mutant (Figure 2C). Neurocalcin δ stimulated its activity with an $EC_{50}$ of 0.8 μM, and the maximal stimulation of about 2.5-fold was obtained at 2 μM neurocalcin δ.

Together, these results lead to the conclusions that the $G^{817}-Y^{965}$ domain of ROS-GC1 constitutes the core catalytic domain, the $Ca^{2+}$-bound neurocalcin δ-modulated site resides in this domain, and the domain is intrinsically active and exists as a dimer. Also, the dd is not obligatory for its activity. The current dogma is that the dd is pivotal for the catalytic activity of all members of the membrane guanylate cyclase family (*46, 47*).

*The Catcd Binds Neurocalcin δ.* To decide if $Ca^{2+}$-bound neurocalcin δ binds directly to catcd, SPR analyses were performed. The catcd fragment, $G^{817}-Y^{965}$, was immobilized on a sensor chip, and incremental concentrations of neurocalcin δ were supplied in the mobile phase. A representative set of sensorgrams with the respective curves derived after fitting to a 1:1 Langmuir binding model is presented (Figure 3A). It is noted that the dissociation phase commenced before the injection was completed, particularly at higher concentrations of neurocalcin δ (Figure 3A, 4 μM). To determine the half-maximal binding ($EC_{50}$), the average experimental RU values at equilibrium ($RU_{eq}$) were plotted as a function of neurocalcin δ concentration (Figure 3B). Half-maximal binding was at 0.5 μM. Analyses of the data using a nonlinear regression curve fit model and by Scatchard plot (Figure 3C) yielded $K_D$ values of 0.66 and 0.7 μM, respectively. When this value was calculated using the BIAevaluation 3.2 software, it was 0.55 μM. These values are comparable, and they are in good agreement with the $EC_{50}$ value for neurocalcin δ activation of catcd (Figure 2C). Thus, the catcd domain of ROS-GC1 defines the neurocalcin δ binding and transduction site.

Other binding parameters between neurocalcin δ and catcd assessed by the SPR analysis were as follows: $k_{on}$ (association rate constant) $7.7 \times 10^4\ M^{-1}\ s^{-1}$, $k_{off}$ (dissociation constant) $4.2 \times 10^{-2}\ s^{-1}$, $K_A$ (equilibrium association constant) $1.8 \times 10^6\ M^{-1}$, and $K_D$ (equilibrium dissociation constant) $5.52 \times 10^{-7}\ M^{-1}$. Thus, binding between ROS-GC1 and neurocalcin δ is of moderate affinity. The values are very close to the previously determined values for the ROS-GC1 fragment aa733−1054 (*16*), leading to the conclusion that the catcd fragment, $G^{817}-Y^{965}$, houses the complete neurocalcin δ binding site.

*Peptide Competition Experiments Define the aa837−858 Region of ROS-GC1 To Be the Binding and the Transduction Site of Neurocalcin δ.* To narrow down the neurocalcin δ regulatory site and to determine if this site is also the transduction site, peptide competition experiments were conducted. Peptides spanning the aa797−961 region, consisting of the entire catcd and the N-terminally located 20 aa domain, were synthesized with a length of 22 aa and an overlap of 2 aa. These peptides were scanned for their inhibitory effects on the neurocalcin δ-dependent ROS-GC1 activity.

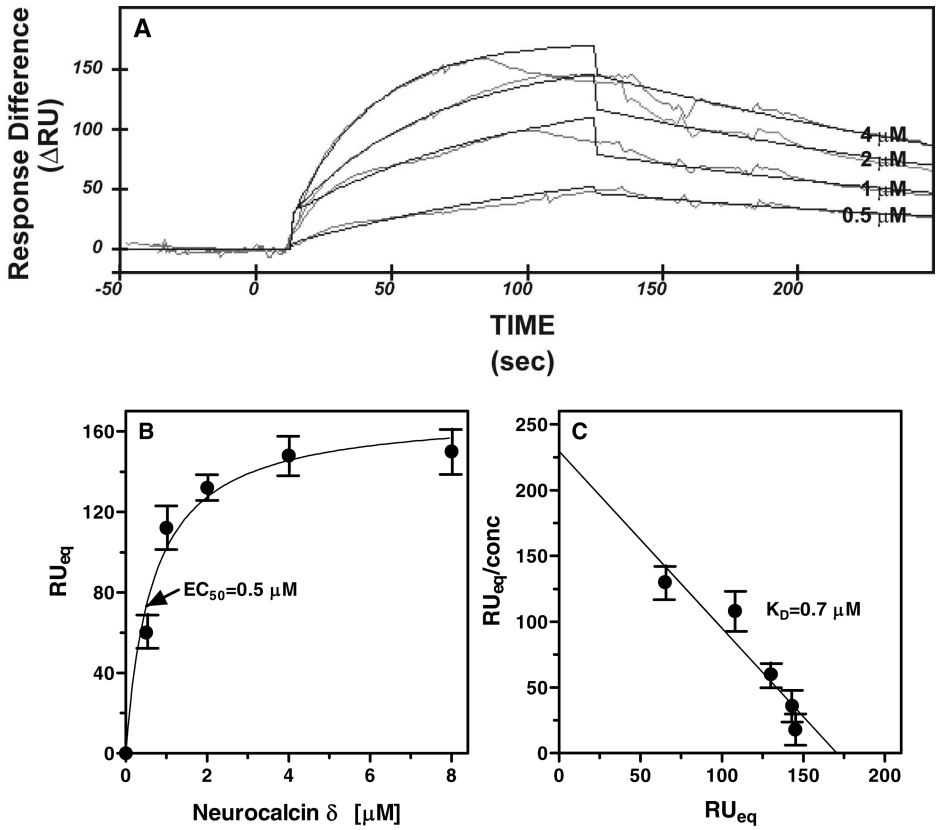


FIGURE 3: Binding of neurocalcin δ to the ROS-GC1 region $G^{817}-Y^{965}$. Purified ROS-GC1 fragment $G^{817}-Y^{965}$ was immobilized on a CM5 sensor chip, and neurocalcin δ was supplied in the mobile phase. (A) A set of four representative sensorgrams from one run depicting binding of neurocalcin δ at concentrations of 0.5, 1, 2, and 4 μM is shown. The curves were fitted to a 1:1 Langmuir model. The raw (in gray) and fitted (in black) curves for each concentration of neurocalcin δ are presented. (B) Binding at equilibrium ($RU_{eq}$) as a function of neurocalcin δ concentration. The results presented are the mean ± standard error of four experiments performed on different days with two independent preparations of neurocalcin δ. The data were analyzed using GraphPad Prism and resulted in an $EC_{50}$ value of 0.5 μM and a $K_D$ value of 0.66 μM. (C) Scatchard transformation of the binding data. Linear regression analysis of the data was carried out with GraphPad Prism.

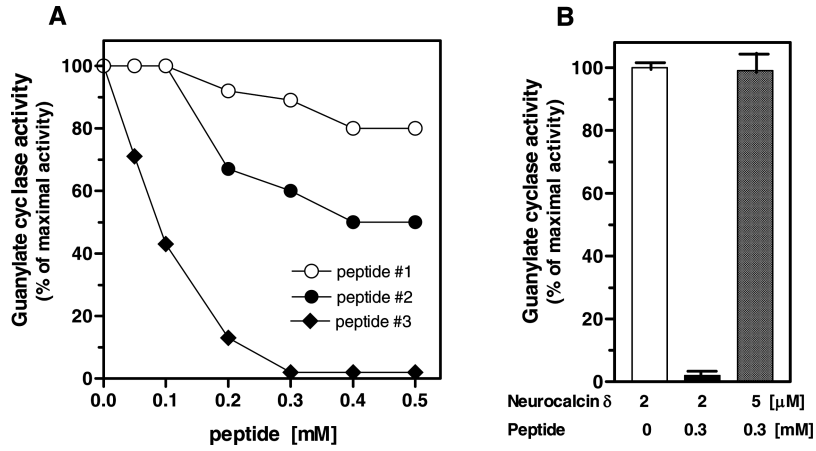


FIGURE 4: Peptide competition. (A) Inhibition of ROS-GC1 activity. Membranes of COS cells expressing ROS-GC1 were incubated with increasing concentrations of a peptide in the presence of 2 μM neurocalcin δ and 100 μM $Ca^{2+}$. (B) Reversal of inhibition by an excess of neurocalcin δ. Membranes of COS cells expressing ROS-GC1 were incubated with 2 μM neurocalcin δ (open bars), 2 μM neurocalcin δ and 0.3 mM peptide (closed bars), or 5 μM neurocalcin δ and 0.3 mM peptide (checkered bars) and assayed for guanylate cyclase activity as in (A). Experiments were carried out in triplicate and repeated twice. The data shown are from a representative experiment.

The COS cell membranes expressing ROS-GC1 were incubated with a 0.4 mM concentration of each peptide in the presence of 2 μM neurocalcin δ and $Ca^{2+}$. Only three peptides significantly inhibited neurocalcin δ-stimulated cyclase activity, and their inhibitory effect was further analyzed. Peptide 3, $^{837}$VGFTTISAMSEPIEVVDLLNDL$^{858}$, was the most effective (Figure 4A). It caused almost complete inhibition at 300 μM, and its $IC_{50}$ value was 90 μM (Figure 4A). Peptide 1, $^{797}$QKTDRLLTQMLPPSVAEALKMG$^{818}$, and peptide 2, $^{817}$MGTPVEPEYFEEVTLYFSDIVG$^{838}$, did not show any inhibition of neurocalcin δ-stimulated activity up to 125 μM. However, they both respectively inhibited 20% and 50% of the neurocalcin δ-dependent activity at 400 μM; their $IC_{50}$ values were 250 and 200 μM (Figure 4A). These results demonstrate that the major neurocalcin δ binding and transduction site resides

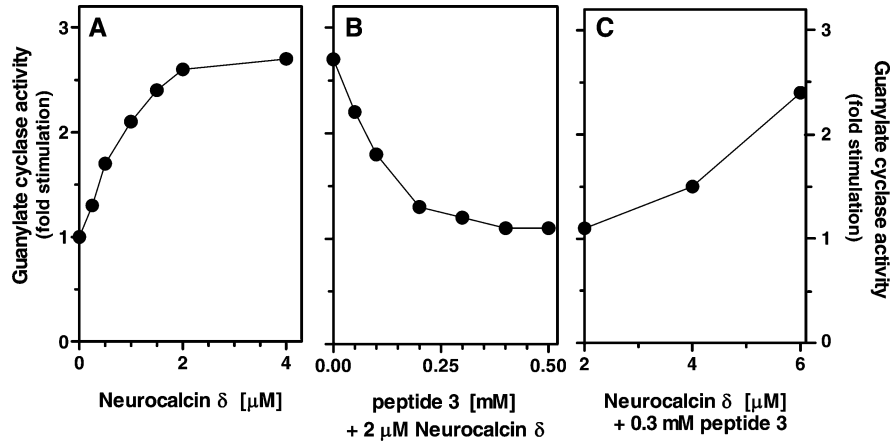


FIGURE 5: Peptide competition on the isolated ROS-GC1 fragment $G^{817}-Y^{965}$. The ROS-GC1 fragment $G^{817}-Y^{965}$ was assayed for neurocalcin $\delta$-dependent cyclase activity in the presence of 100 $\mu$M $Ca^{2+}$ (A). To the reaction mixture consisting of 2 $\mu$M neurocalcin $\delta$, the fragment, and 100 $\mu$M $Ca^{2+}$ were added increased concentrations of peptide 3 ($V^{837}-L^{858}$) (B). To the reaction mixture containing 2 $\mu$M neurocalcin $\delta$, the fragment, and 0.3 mM peptide 3 [conditions as in (B)] were added the indicated concentrations of neurocalcin $\delta$ (C), and the guanylate cyclase activity was assayed. The experiment was done in triplicate and was repeated two times. The results presented are from one experiment. Error bars are within the size of the symbol.

within the $V^{837}-L^{858}$ segment of ROS-GC1. A few overlapping residues of peptide 2, however, slightly affected the binding and transduction activities of neurocalcin $\delta$.

This conclusion was validated by the reconstitution study: an excess of neurocalcin $\delta$ resulted in reversal of the inhibition by peptide 3 (Figure 4B). These results prove that the $V^{837}-L^{858}$ region of ROS-GC1 represents both the binding and the transduction domain of neurocalcin $\delta$.

*The Catcd Domain Region $V^{837}-L^{858}$ Is Directly Modulated by Neurocalcin $\delta$.* To further confirm the above conclusion, a direct reconstitution study using the isolated catcd and neurocalcin $\delta$ was conducted. In the presence of a saturating amount of free $Ca^{2+}$, neurocalcin $\delta$ stimulated catcd in a dose-dependent fashion with an $EC_{50}$ of 0.8 $\mu$M, $V_{max}$ was achieved at 2 $\mu$M, and its maximal stimulation was about 2.5-fold (Figure 5A). The incubation of catcd with increasing concentrations of peptide 3 ($V^{837}-L^{858}$) in the presence of a 2 $\mu$M concentration of neurocalcin $\delta$ and a saturating amount of $Ca^{2+}$ inhibited in excess of 90% catcd activity (Figure 5B), and reversal of the inhibition occurred with an excess of neurocalcin $\delta$ (Figure 5C). Together, these and the earlier reconstitution results unequivocally prove that the $V^{837}-L^{858}$ domain of ROS-GC1 is both the binding and the transduction site of ROS-GC1.

*The $V^{837}-L^{858}$ Signal Transduction Site of Catcd Is Specific to Neurocalcin $\delta$.* An exquisite feature of ROS-GC1 is that it is a bimodal $Ca^{2+}$ signal transduction switch; nanomolar to semimicromolar ranges of free $Ca^{2+}$ stimulate and higher ranges inhibit it. The former mode occurs via GCAPs, 1 and 2; the latter via CD-GCAPs, S100B and neurocalcin $\delta$. To assess the specificity of the neurocalcin $\delta$ signal transduction site, catcd was tested for its responses to GCAPs and S100B; wtROS-GC1 expressed in COS cells served as a positive control.

Both GCAPs and S100B stimulated ROS-GC1 activity, 6-, 5.5-, and 9-fold for GCAP1, GCAP2, and S100B, respectively, but had no influence on the isolated catcd's activity (Figure 6). Therefore, the neurocalcin $\delta$, GCAP1, GCAP2, and S100B modular sites in ROS-GC1 are distinct and totally independent of each other's activity.

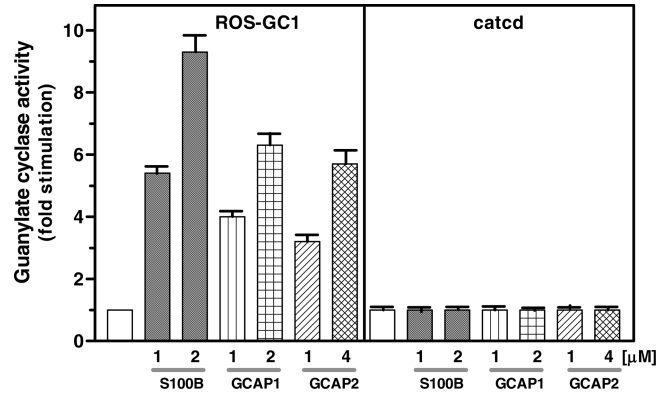


FIGURE 6: Specificity of the catcd $V^{837}-L^{858}$ signal transduction site. The purified catcd fragment was assayed for guanylate cyclase activity in the presence of the indicated concentrations of S100B and 100 $\mu$M $Ca^{2+}$ or GCAP1 or GCAP2 in the presence of 10 nM $Ca^{2+}$. Membranes of COS cell expressing ROS-GC1 were processed in parallel as the control. The experiment was done in triplicate and repeated two times with separate protein preparations. The results presented (mean ± SD) are from one experiment.

*The ROS-GC1 Segment $^{845}$MSEPIE$^{850}$ Is an Important Motif for Neurocalcin $\delta$ Signal Transduction.* Alignment of the ROS-GC1 region $V^{837}-L^{858}$ sequence with the sequence of another ROS-GC subfamily member, ONE-GC (GenBank number L37203), which is also modulated by $Ca^{2+}$-bound neurocalcin $\delta$ (*17–19*), showed a common MSEPIE motif. This motif is not conserved in the natriuretic peptide receptor guanylate cyclases, ANF-RGC and CNP-RGC. In these receptor cyclases, the corresponding sequence is **ESTPMQ** (variant residues indicated in bold). The possibility was considered that the catcd segment $^{845}$MSEPIE$^{850}$ may be important for neurocalcin $\delta$ signaling.

To assess this possibility, the $^{845}$MSEPIE$^{850}$ motif was deleted in the catcd sequence, and the construct, catcdΔMSEPIE (Figure 2A), was purified and analyzed.

Its basal guanylate cyclase activity was identical to its parent catcd (compare 7.1 with 7; Figure 2A). This indicated that the tertiary structure of the mutant has not been affected by the deletion of the motif and the motif has no role in regulation of the basal cyclase activity of the core catalytic module.

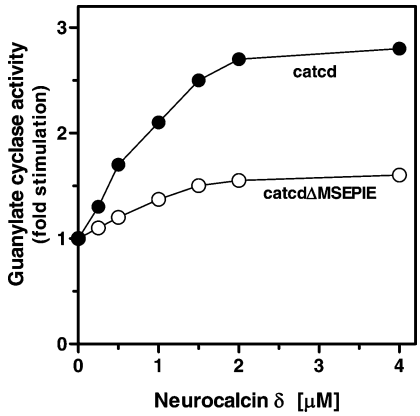


FIGURE 7: Effect of neurocalcin δ on the guanylate cyclase activity of the catcdΔMSEPIE. The catcdΔMSEPIE mutant was assayed for guanylate cyclase activity in the presence of increasing concentrations of neurocalcin δ and 100 μM $Ca^{2+}$. The catcd (control) was treated identically. The experiment was done in triplicate and repeated four times. The results presented are from one experiment. The error bar is within the size of the symbol.

However, the mutant lost 75% of its neurocalcin δ-modulated activity (Figure 7). This concludes that the $^{845}$MSEPIE$^{850}$ motif is essential in the neurocalcin-modulated $Ca^{2+}$ signaling of the catalytic module.

*Molecular Modeling.* To pictorially define the neurocalcin-binding domain in the catalytic module and the neurocalcin δ domain with which the catalytic module interacts, the tools of molecular modeling and docking were used.

For these tasks, in the absence of its crystal structure, a fold recognition based model of the ROS-GC1's catalytic domain was created; for neurocalcin δ, the available crystal structure was used as a template (PDB ID 1BJF; *49*).

A previous study has modeled the three-dimensional structure of the catalytic module of human ROS-GC1 (PDB ID 1AWL; *50*), and using it as a template, a subsequent study has successfully resolved its catalysis sites (*51*). The 1AWL model is very similar to the model in the present study. However, the 1AWL model warrants certain comments.

At the time the 1AWL model was created, the understanding was that membrane guanylate cyclases were active only when dimerized (*47*). They needed the coiled-coil dimerization structural motif for its stepwise activation, first dimer formation to express its basal and subsequently to show its regulatory activities. Therefore, the isolated catalytic domain, lacking the α-helical dd, would be monomeric. These facts were ignored in the construction of the 1AWL model, which depicts the isolated catalytic domain as a dimer. Importantly, the site-directed mutagenesis study conducted to validate the model was on the intact wild-type ROS-GC1 and not on the isolated catalytic domain construct (*51*).

In contrast, the principles on which the present model is built are opposite to those of the 1AWL model. Here the model is built after the properties of the isolated catalytic module without its coiled-coiled structural motif have been established; i.e., the module is intrinsically dimerized, is active, and is inherently regulatory.

*The Neurocalcin δ-Binding Domain Represents a Helix−Loop−Helix Structural Motif.* The template used to create the three-dimensional catcd model was the crystal structure of $G_s$-bound adenylate cyclase II (PDB ID 1AZS; *52*) [rat AC2 $C_2$ domain homodimer was the template for the 1AWL model (*50*)]. The program used in this study was Phyre. It incorporates the secondary structure along with the aa sequence profiles of the protein. The monomer form of the model is presented in Figure 8A; it is referred to as the "modified catcd model" (modified model) to distinguish it from the 1AWL model. The modified model encompasses the $M^{816}$−$L^{1006}$ region of the catalytic domain; notably, the region does not contain the hinge region of ROS-GC1 (dd in Figure 2A).

The cat domain consists of six α helices, 1, 2, 3, 3′, 4, and 5, and of eight β sheets, 1−8 (Figure 8A). The α helix 3′ motif is composed of seven residues, $^{911}$TFRMRHM$^{917}$. The structure of this motif was not identified in the 1AWL model.

The cat domain dimer model (Figure 8B) was created using the 1AZS dimer as a template. In general, this model is very similar to the 1AWL model. Both models depict the configuration of the homodimer to be antiparallel. There, however, are some significant differences in the nature of the residues that mediate dimerization and surround the substrate molecule GTP (Supporting Information).

The highlighted feature of the modified model is that it depicts the neurocalcin δ-modulated domain, $V^{837}$−$L^{858}$. This domain is located near the N-terminal region of the core cat domain. This domain is accessible to the solvent and, importantly, is not buried within the dimer interface. These features make this region available for interaction with neurocalcin δ. One important characteristic of this domain is that it consists of a helix−loop−helix structure (Figure 8B; indicated in yellow and by an arrowhead).

*A Docking Study Defines the Neurocalcin δ and the Catd Interaction Site.* To simulate the interaction site between neurocalcin δ and the catalytic domain, two different docking programs, 3D-Dock and ZDOCK, were independently used (discussed in Supporting Information). In more than 10000 docking solutions, both programs yielded only one and the same result: (1) the catalytic core domain $V^{837}$−$L^{858}$ is the favored region that interacts with neurocalcin δ; (2) the residues in and around the EF1 hand of neurocalcin δ are the primary interaction sites with its target catalytic domain.

The neurocalcin δ-docked catalytic module is depicted in Figure 8C. For simplicity, the figure shows the interaction between the catalytic module and neurocalcin δ, monomer to monomer. The interactive sites are located within the dotted box. The helix−loop−helix ($V^{837}$−$L^{858}$) structure of the catcd is indicated as a blue ribbon.

The model provides important clues on the nature of the docking pocket and the events relating to its creation (Figure 8D). The pocket involves the V-shaped crevice of the neurocalcin δ's EF1 hand. Into this crevice fits the helix−loop−helix $V^{837}$−$L^{858}$ region of the catalytic domain (Figure 8D). The residues forming the crevice are $H^{25}$, $E^{26}$, $Q^{28}$, $E^{29}$, $W^{30}$, $K^{32}$, $G^{33}$, $F^{34}$, $R^{36}$, $D^{37}$, $C^{38}$, $L^{43}$, $E^{47}$, $K^{50}$, $I^{51}$, $Y^{52}$, $N^{54}$, $F^{55}$, and $F^{56}$. They are within a sphere of 4.5 Å from the catcd $V^{837}$−$L^{858}$ region and belong to the EF1 hand of neurocalcin δ, and they form a distinctive patch due to the presence of hydrophobic and charged residues. The prediction is that the nature of this solvent-accessible patch is unique for the interaction between the $Ca^{2+}$-bound neurocalcin δ and the helix−loop−helix structure of the catalytic domain.

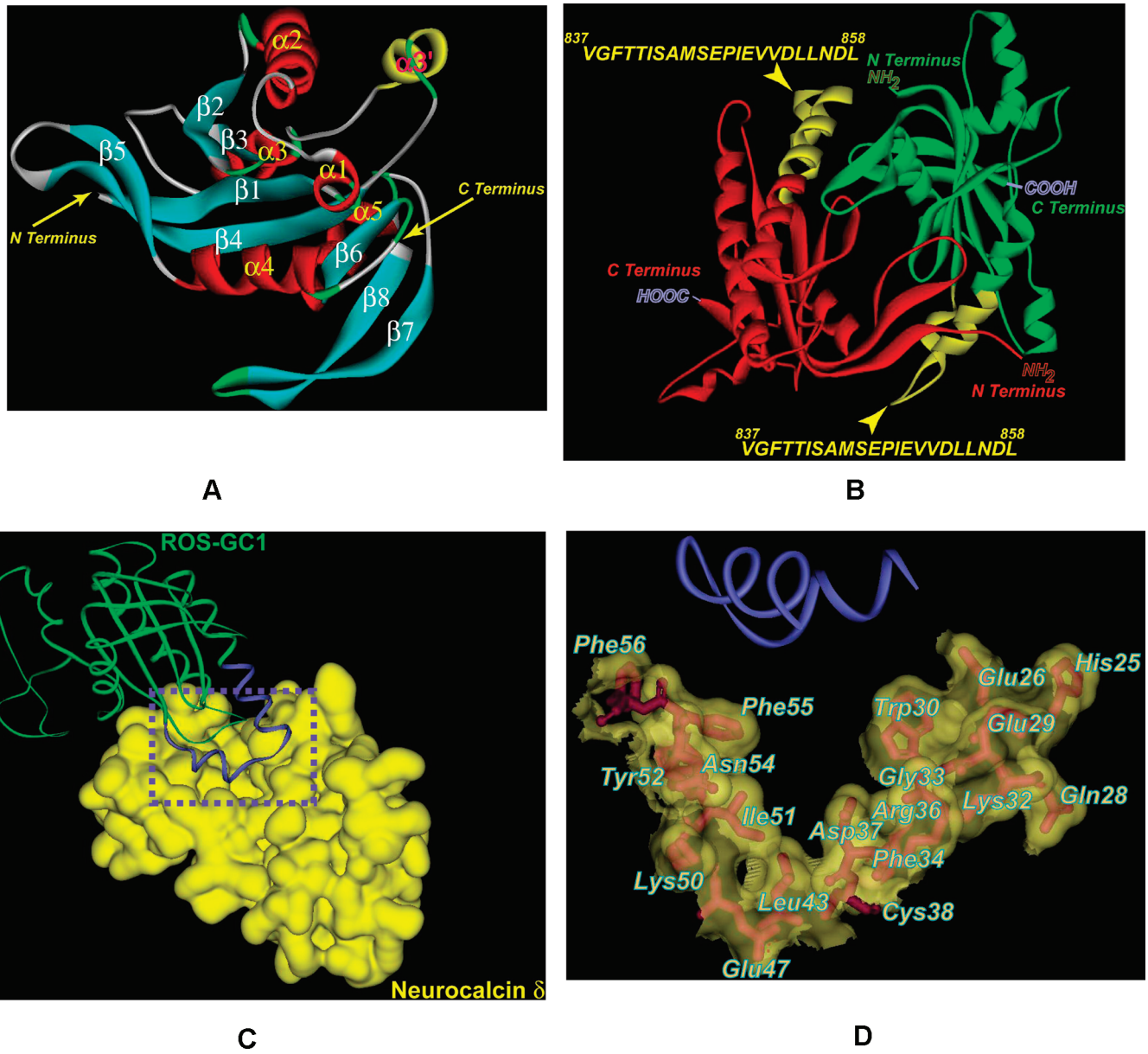


FIGURE 8: Three-dimensional model of the ROS-GC1 catalytic domain and molecular docking of neurocalcin δ. (A) Ribbon diagram of the ROS-GC1 catalytic domain monomer. A three-dimensional model of the ROS-GC1 domain $M^{816}$–$L^{1006}$ was created as described in Materials and Methods. The α helices are shown in red and the β strands in cyan. Numbering is according to the 1AZS template. The N- and C-termini are indicated by arrows. (B) The solvent-accessible $V^{837}$–$L^{858}$ domain of the ROS-GC1 catalytic domain. The two monomeric ROS-GC1 catalytic domains are indicated in red and green, respectively. Within each monomer, the region corresponding to $V^{837}$–$L^{858}$ (peptide 3) is indicated in yellow and labeled. The N- and C-termini are labeled. (C) The ROS-GC1 catalytic domain/neurocalcin δ complex. Monomers of the ROS-GC1 catalytic domain and of neurocalcin δ are depicted for clarity. The ROS-GC1 catalytic domain is depicted as a green ribbon, and its helix–loop–helix $V^{837}$–$L^{858}$ region is in blue; the solvent-accessible surface of neurocalcin δ is depicted in gold. A dotted box is drawn around the region of docking. (D) Residues on neurocalcin δ within a 4.5 Å sphere from the interacting ROS-GC1 catalytic domain region. The docking region [dotted box in (C)] is expanded. The ROS-GC1 helix–loop–helix region ($V^{837}$–$L^{858}$) is depicted as a blue ribbon. The neurocalcin δ residues located within a 4.5 Å sphere from the $V^{837}$–$L^{858}$ region are depicted as stick models in red, embedded within the solvent surface (transparent gold). The amino acid residues are labeled.

## DISCUSSION

In this comprehensive study a new transduction model for the $Ca^{2+}$ signaling of ROS-GC1 is defined. This transduction model is applicable to the cyclic GMP signaling pathway present in the inner plexiform layers of the retinal layers and is modulated by the $Ca^{2+}$ sensor neurocalcin δ (*16, 53, 54*). Molecular principles of this model are illustrated below.

*The Neurocalcin δ-Modulated Site in ROS-GC1 Is Unusual.* The intracellular region of ROS-GC1 is modular in nature, and through defined modules this region acts as the transduction site of multiple forms of $Ca^{2+}$ signals: GCAP1's, $M^{445}$–$L^{456}$ and $L^{503}$–$I^{522}$ (*55*); GCAP2's, $Y^{965}$–$N^{981}$ (*43*); and S100B's, $G^{962}$–$N^{981}$ (*14*).

The present study demonstrates that the $V^{837}$–$L^{858}$ region of ROS-GC1 is the neurocalcin δ binding and also the transduction site in ROS-GC1. This site contains a consensus neurocalcin δ recognition and transduction motif, whose sequence is $^{845}$MSEPIE$^{850}$.

The location of the neurocalcin-modulated site is unusual. Unlike the domains of other $Ca^{2+}$ sensors, this site resides in the core domain of the catalytic module. The residences

of all other modular domains are outside the catalytic domain, and the $Ca^{2+}$ signals modulated by these domains do not interfere with operation of the neurocalcin δ module.

*Boundary of the Catalytic Domain.* The unexpected finding that the neurocalcin δ binding domain resides in the catalytic domain required the resolution of a central issue. What is the precise boundary of the catalytic module in ROS-GC1? This, to date, remains vaguely defined on the basis of the hydropathic analysis of ANF-RGC (reviewed in ref *6*). The entire segment beyond the khd region has been marked as the catalytic cyclase domain (Figure 1 A, top panel).

*The α-Helical Dimerization Structural Element Is Not a Part of the Catalytic Domain.* This region beyond the khd includes an α-helical interdomain, a 43 aa segment, which precedes the catalytic domain (dd in Figure 1A). This segment is conserved in all members of the membrane guanylate cyclase family. The present consensus is that it functions as a dimerization domain for all members of the membrane guanylate cyclase family, and the dd constitutes a pivotal structural component for a unified transduction model of all members of the guanylate cyclase family (*44, 46, 47*). In this theme, the peptide hormone, or the $Ca^{2+}$, signal activates the dd; the dd, in turn, causes dimerization of the catalytic domain, and the dimerization event results in basal and regulatory activities of the catalytic domain.

Implicit in this theme is that the catalytic domain in its native state is monomeric. A critical element of this signal transduction model is that the contact points for dimerization of the core catalytic domain reside in the dd. For the ROS-GC1 model this element is $Arg^{787}$ (*47*). This model has been validated for the ANF signaling of ANF-RGC (*46*) and the GCAP1 signaling of ROS-GC1 (*47*). However, none of these studies have been conducted on the isolated domain of the catalytic domain.

The present study, which incorporates the results of the isolated catalytic module, proves that 45 aa dd is not a part of the catalytic core domain. The core domain is intrinsically active in both its basal and neurocalcin δ regulatory state. In its native state, it exists as a dimer. Finally, because $Arg^{787}$ is not a part of the core catalytic domain, it is not a pivotal element in the neurocalcin δ-modulated ROS-GC signal transduction model. Therefore, the fundamental principles of operation for the neurocalcin δ-modulated ROS-GC1 transduction mechanism are unique to itself.

*ROS-GC1, Three-Dimensional Model.* First, to view its tertiary structure, the fold recognition based model of the monomer of the catalytic module was built. It covered the aa segment 816−1006 of ROS-GC1. A noteworthy feature of this model is that it does not contain the dd domain; this eliminates any effect this domain may have on the structure of the catalytic module. Compared to 1AWL (*50*), this model indicates an additional seven-residue $^{911}$TFRMRHM$^{917}$ helix.

On the basis of the existing evidence that the native form of ROS-GC1 is composed of two homomeric subunits, to pictorially define the neurocalcin-binding transduction motif, $V^{837}$−$L^{858}$, in their respective monomers, the catd dimer model was created.

The prominent feature of this model (Figure 8B) is that two chains of the catalytic module are antiparallel. In each chain, the neurocalcin δ-binding transduction motif is located toward the N-terminal region of the chain. In these configurations, the two neurocalcin-binding transduction sites are distally apart. The notable characteristics of these sites are that they are composed of helix−loop−helix structure (Figure 8B, yellow ribbons).

*Catalytic Domain Neurocalcin δ Interaction Site.* A remarkable result of the modeling-docking study is that it explains the principles of the union between the catalytic domain of ROS-GC1 and neurocalcin δ. The contact points between these domains are designed to form a perfect fit. The neurocalcin δ-binding transduction motif of the catalytic domain consists of a helix−loop−helix structure (Figure 8B). This structure is accessible to the solvent and comfortably fits in the V-shaped crevice of neurocalcin δ. This crevice is formed by the defined EF1-hand residues (Figure 8D). These residues form a special hydrophobic−hydrophilic patch, which may be a distinctive feature of the $Ca^{2+}$-dependent signaling property of neurocalcin δ.

*Signal Transduction Model.* By the facts provided by this study and some aided by the computational modeling, a preliminary stepwise neurocalcin δ signal transduction model is envisioned. Step 1: the postphototransduction signal in the IPL neurons generates a rise of free $Ca^{2+}$ in the semimicromolar range. Step 2: $Ca^{2+}$ binds neurocalcin δ. Step 3: neurocalcin δ undergoes a $Ca^{2+}$-dependent configurational change. Step 4: with an $EC_{50}$ of 0.5 μM, its defined domain in the EF1 hand binds its $V^{837}$−$L^{858}$ modulated region of the cat domain in ROS-GC1; the cat domain in its native form exists as a dimer. Step 5: with $k_{on}$ of $7 \times 10^4$ $M^{-1}$ $s^{-1}$, the cat domain is activated and generates cyclic GMP. Step 6: with a $k_{off}$ of $4.2 \times 10^{-2}$ $s^{-1}$, the neurocalcin is dissociated, and the process reverts back to the step 1 state of the neuron.

Similar operational steps are envisioned in the neurocalcin δ-modulated $Ca^{2+}$ signaling of the ONE-GC membrane guanylate cyclase in the olfactory neuroepithelium linked with the odorant transduction (*19*).

## SUPPORTING INFORMATION AVAILABLE

The technical details related to modeling and docking procedures such as the parameters used in the creation of the model and docked complexes, analyses regarding the model with respect to its substrate- (GTP-) binding site and dimerization, and analyses regarding the residues on ROS-GC1 and neurocalcin δ that mediate the interaction. This material is available free of charge via the Internet at http://pubs.acs.org.

## REFERENCES

1. Paul, A. K. (1986) Doctoral Thesis, University of Tennessee.
2. Paul, A. K., Marala, R. B., Jaiswal, R. K., and Sharma, R. K. (1987) Coexistence of guanylate cyclase and atrial natriuretic factor receptor in a 180-kD protein. *Science 235*, 1224–1226.
3. Kuno, T., Andersen, J. W., Kamisaki, T., Waldman, S. A., Chang, L. Y., Saheki, S., Leitman, D. C., Nakane, M., and Murad, F. (1986) Co-purification of an atrial natriuretic factor receptor and particulate guanylate cyclase from rat lung. *J. Biol. Chem. 261*, 5817–5823.
4. Margulis, A., Goraczniak, R., Duda, T., Sharma, R. K., and Sitaramayya, A. (1993) Structural and biochemical identity of retinal rod outer segment membrane guanylate cyclase. *Biochem. Biophys. Res. Commun. 194*, 855–861.
5. Goraczniak, R., Duda, T., Sitaramayya, A., and Sharma, R. K. (1994) Structural and functional characterization of the rod outer segment membrane guanylate cyclase. *Biochem. J. 302*, 455–461.
6. Sharma, R. K. (2002) Evolution of the membrane guanylate cyclase transduction system. *Mol. Cell. Biochem. 230*, 3–30.

7. Pugh, E. N., Jr., Duda, T., Sitaramayya, A., and Sharma, R. K. (1997) Photoreceptor guanylate cyclases: a review. *Biosci. Rep. 17*, 429–473.
8. Koch, K.-W., Duda, T., and Sharma, R. K. (2002) Photoreceptor specific guanylate cyclases in vertebrate phototransduction. *Mol. Cell. Biochem. 230*, 97–106.
9. Sharma, R. K., Duda, T., Venkataraman, V., and Koch, K.-W. (2004) Calcium-modulated membrane guanylate cyclase, ROS-GC transduction machinery in sensory neurons: a universal concept. *Curr. Top. Biochem. Res. 6*, 111–144.
10. Schulz, S., Green, C. K., Yuen, P. S., and Garbers, D. L. (1990) Guanylyl cyclase is a heat-stable enterotoxin receptor. *Cell 3*, 941–948.
11. Koller, K. J., Lowe, D. G., Bennett, G. L., Minamino, N., Kangawa, K., Matsuo, H., and Goeddel, D. V. (1991) Selective activation of the B natriuretic peptide receptor by C-type natriuretic peptide (CNP). *Science 252*, 120–123.
12. Duda, T., Goraczniak, R., Sitaramayya, A., and Sharma, R. K. (1993) Cloning and expression of an ATP-regulated human retina C-type natriuretic factor receptor guanylate cyclase. *Biochemistry 32*, 1391–1395.
13. Koch, K.-W., and Stryer, L. (1988) Highly cooperative feedback control of retinal rod guanylate cyclase by calcium ions. *Nature 334*, 64–66.
14. Duda, T., Koch, K.-W., Venkataraman, V., Lange, C., Beyermann, M., and Sharma, R. K. (2002) Ca(2+) sensor S100beta-modulated sites of membrane guanylate cyclase in the photoreceptor-bipolar synapse. *EMBO J. 21*, 2547–2556.
15. Venkataraman, V., Duda, T., Vardi, N., Koch, K.-W., and Sharma, R. K. (2003) Calcium-modulated guanylate cyclase transduction machinery in the photoreceptor-bipolar synaptic region. *Biochemistry 42*, 5640–5648.
16. Krishnan, A., Venkataraman, V., Fik-Rymarkiewicz, E., Duda, T., and Sharma, R. K. (2004) Structural, biochemical, and functional characterization of the calcium sensor neurocalcin delta in the inner retinal neurons and its linkage with the rod outer segment membrane guanylate cyclase transduction system. *Biochemistry 43*, 2708–2723.
17. Duda, T., Jankowska, A., Venkataraman, V., Nagele, R. G., and Sharma, R. K. (2001) A novel calcium-regulated membrane guanylate cyclase transduction system in the olfactory neuroepithelium. *Biochemistry 40*, 12067–12077.
18. Duda, T., Fik-Rymarkiewicz, E., Venkataraman, V., Krishnan, A., and Sharma, R. K. (2004) Calcium-modulated ciliary membrane guanylate cyclase transduction machinery: constitution and operational principles. *Mol. Cell. Biochem. 267*, 107–122.
19. Duda, T., and Sharma, R. K. (2008) ONE-GC membrane guanylate cyclase, a trimodal odorant signal transducer. *Biochem. Biophys. Res. Commun. 367*, 440–445.
20. Duda, T., and Sharma, R. K. (2004) S100B-modulated $Ca^{2+}$-dependent ROS-GC1 transduction machinery in the gustatory epithelium: a new mechanism in gustatory transduction. *FEBS Lett. 577*, 393–398.
21. Fik-Rymarkiewicz, E., Duda, T., and Sharma, R. K. (2006) Novel frequenin-modulated $Ca^{2+}$-signaling membrane guanylate cyclase (ROS-GC) transduction pathway in bovine hippocampus. *Mol. Cell. Biochem. 291*, 187–204.
22. Venkataraman, V., Nagele, R., Duda, T., and Sharma, R. K. (2000) Rod outer segment membrane guanylate cyclase type 1-linked stimulatory and inhibitory calcium signaling systems in the pineal gland: biochemical, molecular, and immunohistochemical evidence. *Biochemistry 39*, 6042–6052.
23. Jankowska, A., Burczynska, B., Duda, T., Warchol, J. B., and Sharma, R. K. (2007) Calcium-modulated rod outer segment membrane guanylate cyclase type 1 transduction machinery in the testes. *J. Androl. 28*, 50–58.
24. Gorczyca, W. A., Gray-Keller, M., Detwiler, P. B., and Palczewski, K. (1994) Purification and physiological evaluation of a guanylate cyclase activating protein from retinal rods. *Proc. Natl. Acad. Sci. U.S.A. 91*, 4014–4018.
25. Dizhoor, A. M., Olshevskaya, E. V., Henzel, W. J., Wong, S. C., Stults, J. T., Ankoudinova, I., and Hurley, J. B. (1995) Cloning, sequencing, and expression of a 24-kDa $Ca^{2+}$-binding protein activating photoreceptor guanylyl cyclase. *J. Biol. Chem. 270*, 25200–25206.
26. Frins, S., Bonigk, W., Muller, F., Kellner, R., and Koch, K.-W. (1996) Functional characterization of a guanylyl cyclase-activating protein from vertebrate rods. Cloning, heterologous expression, and localization. *J. Biol. Chem. 271*, 8022–8027.
27. Krishnan, A., Goraczniak, R. M., Duda, T., and Sharma, R. K. (1998) Third calcium-modulated rod outer segment membrane guanylate cyclase transduction mechanism. *Mol. Cell. Biochem. 178*, 251–259.
28. Imanishi, Y., Li, N., Sokal, I., Sowa, M. E., Lichtarge, O., Wensel, T. G., Saperstein, D. A., Baehr, W., and Palczewski, K. (2002) Characterization of retinal guanylate cyclase-activating protein 3 (GCAP3) from zebrafish to man. *Eur. J. Neurosci. 15*, 63–78.
29. Margulis, A., Pozdnyakov, N., and Sitaramayya, A. (1996) Activation of bovine photoreceptor guanylate cyclase by S100 proteins. *Biochem. Biophys. Res. Commun. 218*, 243–247.
30. Duda, T., Goraczniak, R., and Sharma, R. K. (1996) Molecular characterization of S100A1-S100B protein in retina and its activation mechanism of bovine photoreceptor guanylate cyclase. *Biochemistry 35*, 6263–6266.
31. Pozdnyakov, N., Goraczniak, R., Margulis, A., Duda, T., Sharma, R. K., Yoshida, A., and Sitaramayya, A. (1997) Structural and functional characterization of retinal calcium-dependent guanylate cyclase activator protein (CD-GCAP): identity with S100beta protein. *Biochemistry 36*, 14159–14166.
32. Kumar, V. D., Vijay-Kumar, S., Krishnan, A., Duda, T., and Sharma, R. K. (1999) A second calcium regulator of rod outer segment membrane guanylate cyclase, ROS-GC1: neurocalcin. *Biochemistry 38*, 12614–12620.
33. Lowe, D. G., Dizhoor, A. M., Liu, K., Gu, Q., Spencer, M., Laura, R., Lu, L., and Hurley, J. B. (1995) Cloning and expression of a second photoreceptor-specific membrane retina guanylyl cyclase (RetGC), RetGC-2. *Proc. Natl. Acad. Sci. U.S.A. 92*, 5535–9553.
34. Goraczniak, R., Duda, T., and Sharma, R. K. (1997) Structural and functional characterization of a second subfamily member of the calcium-modulated bovine rod outer segment membrane guanylate cyclase, ROS-GC2. *Biochem. Biophys. Res. Commun. 234*, 666–670.
35. Fülle, H. J., Vassar, R., Foster, D. C., Yang, R. B., Axel, R., and Garbers, D. L. (1995) A receptor guanylyl cyclase expressed specifically in olfactory sensory neurons. *Proc. Natl. Acad. Sci. U.S.A. 92*, 3571–3575.
36. Dizhoor, A. M., Lowe, D. G., Olshevskaya, E. V., Laura, R. P., and Hurley, J. B. (1994) The human photoreceptor membrane guanylyl cyclase, RetGC, is present in outer segments and is regulated by calcium and a soluble activator. *Neuron 12*, 1345–1352.
37. Duda, T., Goraczniak, R., Surgucheva, I., Rudnicka-Nawrot, M., Gorczyca, W. A., Palczewski, K., Sitaramayya, A., Baehr, W., and Sharma, R. K. (1996) Calcium modulation of bovine photoreceptor guanylate cyclase. *Biochemistry 35*, 8478–8482.
38. Duda, T., Venkataraman, V., Krishnan, A., Nagele, R. G., and Sharma, R. K. (2001) Negatively calcium-modulated membrane guanylate cyclase signaling system in the rat olfactory bulb. *Biochemistry 40*, 4654–4662.
39. Duda, T., Krishnan, R., and Sharma, R. K. (2006) GCAP1: Antithetical calcium sensor of ROS-GC transduction machinery. *Calcium Binding Protein 1*, 102–107.
40. Nambi, P., Aiyar, N. V., and Sharma, R. K. (1982) Adrenocorticotropin-dependent particulate guanylate cyclase in rat adrenal and adrenocortical carcinoma: comparison of its properties with soluble guanylate cyclase and its relationship with ACTH-induced steroidogenesis. *Arch. Biochem. Biophys. 217*, 638–646.
41. Kelley, L. A., MacCallum, R. M., and Sternberg, M. J. (2000) Enhanced genome annotation using structural profiles in the program 3D-PSSM. *J. Mol. Biol. 299*, 499–520.
42. Gribskov, M., McLachlan, A. D., and Eisenberg, D. (1987) Profile analysis: Detection of distantly related proteins. *Proc. Natl. Acad. Sci. U.S.A. 84*, 4355–4358.
43. Duda, T., Fik-Rymarkiewicz, E., Venkataraman, V., Krishnan, R., Koch, K.-W., and Sharma, R. K. (2005) The calcium-sensor guanylate cyclase activating protein type 2 specific site in rod outer segment membrane guanylate cyclase type 1. *Biochemistry 44*, 7336–7345.
44. Garbers, D. L. (1992) Guanylyl cyclase receptors and their endocrine, paracrine, and autocrine ligands. *Cell 71*, 1–4.
45. Duda, T., Goraczniak, R., and Sharma, R. K. (1991) Site-directed mutational analysis of a membrane guanylate cyclase cDNA reveals the atrial natriuretic factor signaling site. *Proc. Natl. Acad. Sci. U.S.A. 88*, 7882–7886.
46. Wilson, E. M., and Chinkers, M. (1995) Identification of sequences mediating guanylyl cyclase dimerization. *Biochemistry 34*, 4696–4701.

47. Ramamurthy, V., Tucker, C., Wilkie, S. E., Daggett, V., Hunt, D. M., and Hurley, J. B. (2001) Interactions within the coiled-coil domain of RetGC-1 guanylyl cyclase are optimized for regulation rather than for high affinity. *J. Biol. Chem. 276*, 26218–26229.
48. Duda, T., Venkataraman, V., Jankowska, A., Lange, C., Koch, K.-W., and Sharma, R. K. (2000) Impairment of the rod outer segment membrane guanylate cyclase dimerization in a cone-rod dystrophy results in defective calcium signaling. *Biochemistry 39*, 12522–12533.
49. Vijay-Kumar, S., and Kumar, V. D. (1999) Crystal structure of recombinant bovine neurocalcin. *Nat. Struct. Biol. 6*, 80–88.
50. Liu, Y., Ruoho, A. E., Rao, V. D., and Hurley, J. H. (1997) Catalytic mechanism of the adenylyl and guanylyl cyclases: modeling and mutational analysis. *Proc. Natl. Acad. Sci. U.S.A. 94*, 13414–13419.
51. Tucker, C. L., Hurley, J. M., Miller, T. M., and Hurley, J. B. (1998) Two amino acid substitutions convert a guanylyl cyclase, RetGC-1, into an adenylyl cyclase. *Proc. Natl. Acad. Sci. U.S.A. 95*, 5993–5997.
52. Tesmer, J. J., Sunahara, R. K., Gilman, A. G., and Sprang, S. R. (1997) Crystal structure of the catalytic domains of adenylyl cyclase in a complex with Gsalpha·GTPgammaS. *Science 278*, 1907–1916.
53. Sharma, R. K., and Duda, T. (2006) Calcium sensor neurocalcin δ-modulated ROS-GC transduction machinery in the retinal and olfactory neurons. *Calcium Binding Proteins 1*, 7–11.
54. Duda, T., Venkataraman, V., and Sharma, R. K. (2007) Vision and odorant-linked neurocalcin δ-dependent $Ca^{2+}$-modulated machinery: Constitution and operational principles, in *Neuronal calcium sensor proteins* (Phillippov, P., and Koch, K.-W., Eds.) pp 91−113, Nova Science Publishers, Hauppage, NY.
55. Lange, C., Duda, T., Beyermann, M., Sharma, R. K., and Koch, K.-W. (1999) Regions in vertebrate photoreceptor guanylyl cyclase ROS-GC1 involved in Ca(2+)-dependent regulation by guanylyl cyclase-activating protein GCAP-1. *FEBS Lett. 460*, 27–31.

BI800394S